



OPEN ACCESS

EDITED BY
Guangzhao Wang,
Yangtze Normal University, China

REVIEWED BY
Shuyuan Xiao,
Nanchang University, China
Kai Ren,
Nanjing Forestry University, China

*CORRESPONDENCE
Yong Tang,
20202127@huanghuai.edu.cn

SPECIALTY SECTION
This article was submitted to Theoretical
and Computational Chemistry,
a section of the journal
Frontiers in Chemistry

RECEIVED 19 September 2022
ACCEPTED 29 September 2022
PUBLISHED 19 October 2022

CITATION
Liu M, Tang Y, Yao H, Bai L, Song J and
Ma B (2022), Theoretical study on
photocatalytic performance of ZnO/
C₂N heterostructure towards high
efficiency water splitting.
Front. Chem. 10:1048437.
doi: 10.3389/fchem.2022.1048437

COPYRIGHT
© 2022 Liu, Tang, Yao, Bai, Song and Ma.
This is an open-access article
distributed under the terms of the
[Creative Commons Attribution License
\(CC BY\)](https://creativecommons.org/licenses/by/4.0/). The use, distribution or
reproduction in other forums is
permitted, provided the original
author(s) and the copyright owner(s) are
credited and that the original
publication in this journal is cited, in
accordance with accepted academic
practice. No use, distribution or
reproduction is permitted which does
not comply with these terms.

Theoretical study on photocatalytic performance of ZnO/C₂N heterostructure towards high efficiency water splitting

Meiping Liu^{1,2}, Yong Tang^{2,3*}, Haizi Yao³, Liuyang Bai³,
Jun Song³ and Benyuan Ma³

¹Henan Key Laboratory of Smart Lighting, Huanghuai University, Zhumadian, Henan, China, ²School of Materials Science and Engineering, Xiangtan University, Xiangtan, Hunan, China, ³School of Energy Engineering, Huanghuai University, Zhumadian, Henan, China

The construction of van der Waals heterostructures offers effective boosting of the photocatalytic performance of two-dimensional materials. In this study, which uses the first-principles method, the electronic and absorptive properties of an emerging ZnO/C₂N heterostructure are systematically explored to determine the structure's photocatalytic potential. The results demonstrate that ZnO and C₂N form a type-II band alignment heterostructure with a reduced band gap, and hence superior absorption in the visible region. Furthermore, the band edge positions of a ZnO/C₂N heterostructure meet the requirements for spontaneous water splitting. The ZnO/C₂N heterostructure is known to possess considerably improved carrier mobility, which is advantageous in the separation and migration of carriers. The Gibbs free energy calculation confirms the high catalytic activity of the ZnO/C₂N heterostructure for water-splitting reactions. All the aforementioned properties, including band gap, band edge positions, and optical absorption, can be directly tuned using biaxial lateral strain. A suitable band gap, decent band edge positions, high catalytic activity, and superior carrier mobility thus identify a ZnO/C₂N heterostructure as a prominent potential photocatalyst for water splitting.

KEYWORDS

ZnO/C₂N heterostructure, first-principles method, type-II band alignment, water splitting, carrier mobility, strain

Introduction

The splitting of water into hydrogen (H₂) and oxygen (O₂) under the action of a photocatalyst has attracted extensive interest for its potential in tackling crises of energy and environmental pollution. Apart from the two basic requirements for band gap and band-edge positions, (Fujishima and Honda, 1972), excellent light absorption, low carrier recombination, and considerable carrier mobility are also necessary for a superior

photocatalyst (Li et al., 2016). Extensive experimental and theoretical studies have been conducted to explore efficient novel photocatalysts.

In recent years, emerging two-dimensional (2D) materials have opened up a colorful stage for the design of new photocatalysts (Fan et al., 2021; Ren et al., 2022a; Qin et al., 2022). Notably, the naturally high surface area of 2D materials can provide more active sites for catalytic reactions (Ganguly et al., 2019). Furthermore, 2D materials shorten the migration distance of photogenerated carriers, thereby reducing the recombination of an electron–hole pair (Fan et al., 2021). A large number of 2D materials have been developed for photocatalysis, such as transition-metal dichalcogenide (Voiry et al., 2016), MXene (Cheng et al., 2019), carbonitrides (Wang et al., 2009), and others (Roger et al., 2017). In 2015, Mohammed et al. synthesized a new 2D multifunctional material C_2N with a band gap of 1.96 eV (Mahmood et al., 2015). The C_2N monolayer possesses phonon modes close to those of graphenes (Sahin, 2015), indicating its fine thermal stability. Many facts confirm the highly tunable photocatalytic ability of monolayered C_2N for water splitting (Xu et al., 2015; Ashwin Kishore and Ravindran, 2017). However, the rapid recombination of photogenerated carriers is still a serious issue for the use of the C_2N monolayer in water splitting (Xu et al., 2015).

Some engineering processes have been proposed to improve the photocatalytic performance of monolayer C_2N for water splitting, including doping (Du et al., 2016), defects (Zhang et al., 2018), atomic adsorption (Kishore et al., 2019; Zhang et al., 2022), and strain (Guan et al., 2015). More recently, nascent van der Waals (vdW) heterostructures (Ye et al., 2019; Zhao et al., 2021; Wang et al., 2022) have also been widely considered as a means of promoting the photocatalytic water-splitting performance of the C_2N monolayer. The vdW heterostructure, composed of different 2D components, can maintain the excellent properties of those components, while some novel properties may be generated due to the interlayer coupling effects (Novoselov et al., 2016). Notably, the electron–hole pair, separated on the constituent monolayers, can substantially reduce the recombination rate of carriers, which is indeed favorable for photocatalytic water splitting (Deng et al., 2016; Novoselov et al., 2016). Kumar found that the carrier mobilities of the C_2N/WS_2 heterostructure with photocatalytic potential are efficiently enhanced (Kumar et al., 2018). Theoretical studies reveal that the $C_2N/GaTe$, $C_2N/InTe$, and $C_2N/InSe$ heterostructures are all suitable for photocatalysis, while their photocatalytic properties are sensitive to strain (Wang et al., 2019; Wang X. et al., 2020). The vdW heterostructures, such as the $C_2N/Janus$ monochalcogenides (Ma et al., 2021), CdS/C_2N (Luo et al., 2017), and $h-BN/C_2N$ (Wang G. et al., 2020), are also predicted to have excellent photocatalytic performance. Recently, the novel ZnO/C_2N heterostructure with a direct band gap of 2.0 eV has been reported, and its optoelectronic properties can be tuned with

vertical strain and an external electric field (Song et al., 2021). Monolayered ZnO with its graphene-like structure is a 2D photocatalytic material with high carrier mobility. However, its large band gap (~ 3.3 eV) (Ren et al., 2020) leads to poor absorption, limiting its photocatalytic application. Perhaps the ZnO/C_2N heterostructure formed by two photocatalysts has more prominent carrier mobility and photocatalytic performance, but this remains unknown thus far.

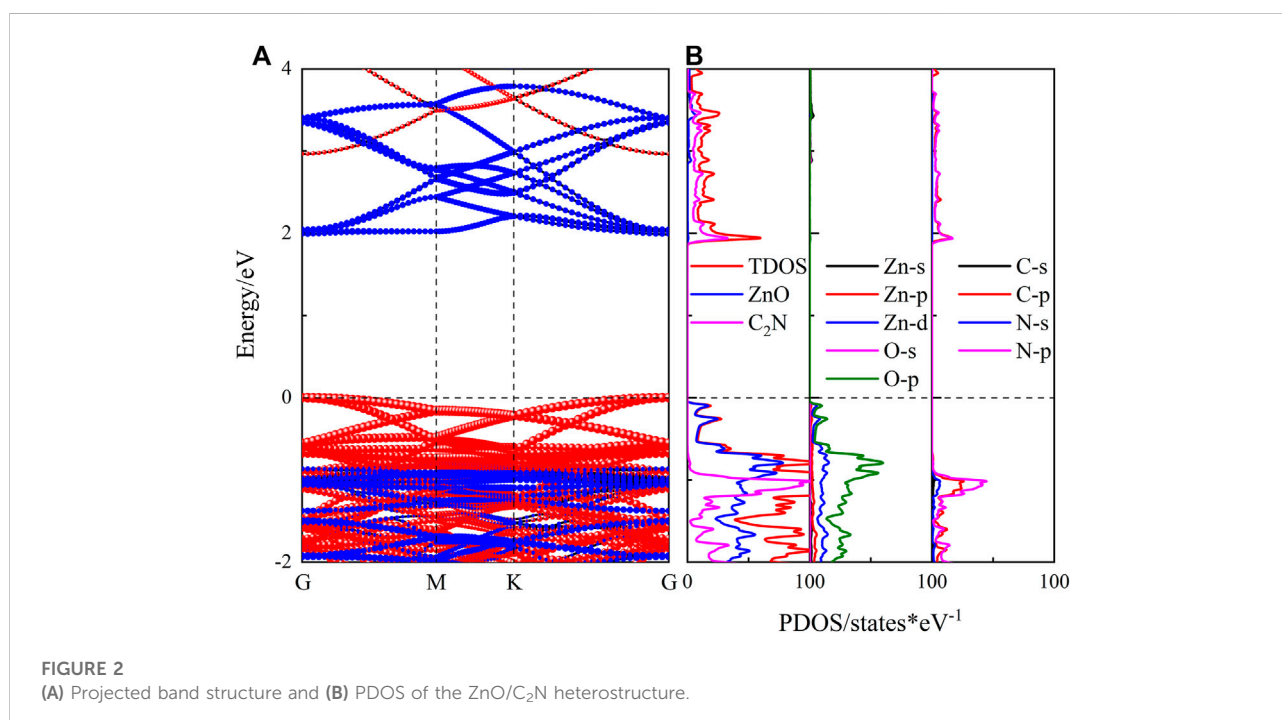
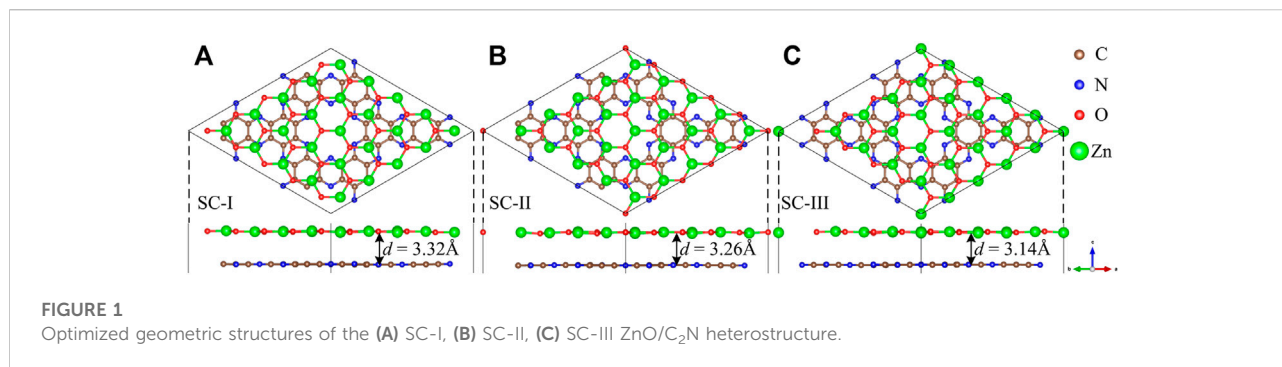
In this work, theoretical work is conducted to comprehensively explore the electronic structure, carrier mobility, hydrogen evolution reaction (HER), and absorption properties of the ZnO/C_2N heterostructure, as well as the effect of lateral strain on these properties. All the results confirm the substantial application potential of a ZnO/C_2N heterostructure in photocatalysis for water splitting.

Computational methods

All calculations are implemented with the Vienna Ab-initio Simulation Package (VASP), based on the projected augmented wave method (PAW) (Kresse and Furthmüller, 1996a; Kresse and Furthmüller, 1996b). The generalized gradient approximation within the Perdew–Burke–Ernzerhof scheme (GGA-PBE) is used to describe the exchange–correlation functional (Perdew et al., 1996), while the DFT-D3 correction method (Grimme et al., 2010) is utilized to describe the vdW interaction between the two monolayers. The Heyd–Scuseria–Ernzerh hybrid functional (HSE06) (Heyd et al., 2003) is also adopted to determine the band gap of the ZnO/C_2N heterostructure and its pristine components. The lattice constants and atomic positions of pristine ZnO and C_2N monolayers are fully relaxed using the $6 \times 6 \times 1$ and $15 \times 15 \times 1$ G -centered Monkhorst–Pack (Monkhorst and Pack, 1976) k -mesh scheme to simplify the Brillouin zone, while a $3 \times 3 \times 1$ k -mesh sampling is chosen for the ZnO/C_2N heterostructure. All ion relaxation processes interrupt the process until the force per atom is less than 0.01 eV/Å and the energy convergence criterion of 10^{-5} eV is set. The plane wave cutoff of 450 eV is used throughout this work, and a 20 Å vacuum toward the z -direction is applied to shield interaction between neighboring layers. VASPKIT and VESTA are used for visualization (Momma and Izumi, 2011; Wang et al., 2021).

Results and discussions

The geometric structures of ZnO and C_2N monolayers are shown in Supplementary Figures S1A–C. Their lattice parameters are found to be 3.29 Å and 8.32 Å, respectively, which is consistent with previous reports (Mahmood et al., 2015; Lee et al., 2016). Both monolayers are direct band gap semiconductors, as the band structures are presented in



Supplementary Figures S1B–D. The band gap values of ZnO and C₂N determined by HSE06 are 3.28 eV and 2.47 eV, which are close to the reported results (Mahmood et al., 2015; Lee et al., 2016).

In order to minimize the strain effect, a 5×5 ZnO supercell and a 2×2 C₂N supercell are used to make up the ZnO/C₂N heterostructure. The ZnO/C₂N heterostructure is constructed by fixing the C₂N layer and shifting the ZnO layer to a high symmetry location. According to the location of the ZnO layer in the lattice, three kinds of stacking configurations (SCs) for the ZnO/C₂N heterostructure are formed, as shown in Figure 1. In the interests of thermodynamic stability and for determining the most stable SC of the ZnO/C₂N heterostructure, the binding energy E_b and the formation energy E_f are calculated using the Supplementary Equations S1, S2. According to the

results in Supplementary Table S1, E_f and E_b are close to those of typical vdW heterostructures (Guo et al., 2017; Fan et al., 2019; Bafekry et al., 2020; Guo et al., 2020). The negative values confirm that all ZnO/C₂N heterostructures can be prepared experimentally, as their stabilities are slightly different. The ZnO/C₂N heterostructure in SC-III, with an interlayer distance d of 3.14 Å, is provided with the most beneficial stability. Therefore, the ZnO/C₂N heterostructure in SC-III is the focus of the following research. Moreover, the *ab initio* molecular dynamic (AIMD) simulation is performed at 300 K to check the thermodynamic stability of the ZnO/C₂N heterostructure. As the snapshot for the last frame shows in Supplementary Figure S3A, the ZnO/C₂N heterostructure maintains good structural integrity within 6 ps, demonstrating its stability at room temperature. The time-dependent evolution of total potential

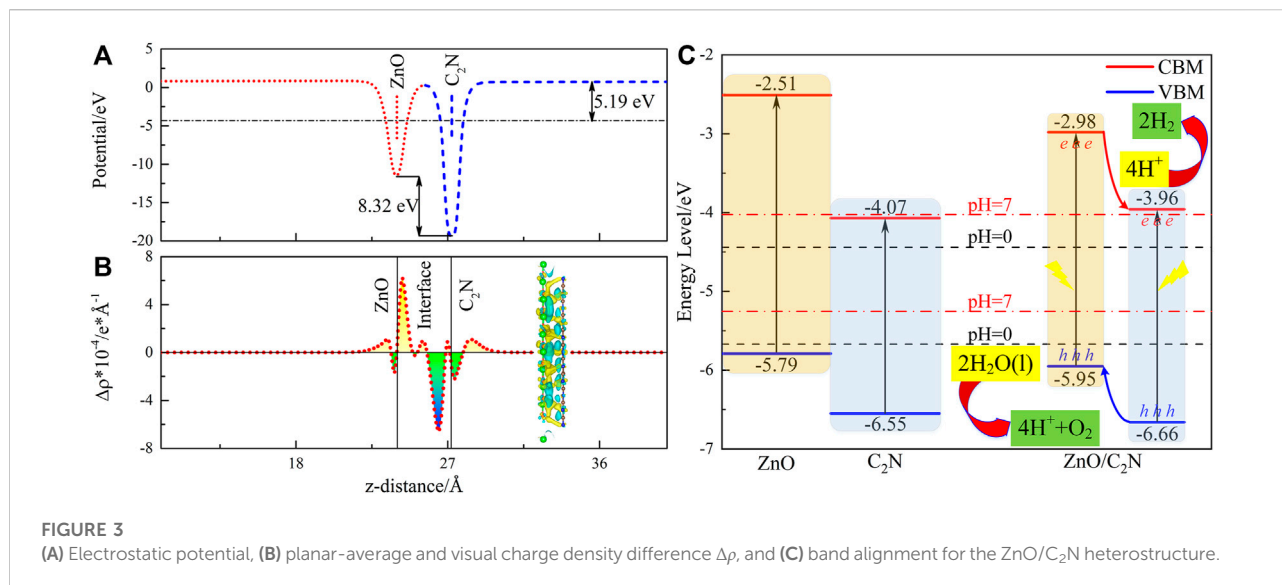


FIGURE 3 (A) Electrostatic potential, (B) planar-average and visual charge density difference $\Delta\rho$, and (C) band alignment for the ZnO/C₂N heterostructure.

energies, exhibited in [Supplementary Figure S3B](#), also proves its thermal stability.

The band structures of the ZnO/C₂N heterostructure within the three SCs are calculated, together with the projected density of states (PDOS). As shown in [Figure 2A](#), the ZnO/C₂N heterostructure is a direct band gap semiconductor, as both the VBM and CBM emerge at the G-point. Results of band structures also indicate that the SC has a negligible impact on electronic property. ZnO/C₂N heterostructures in three SCs possess the same band gap of 0.77 eV and 1.99 eV, based on the PBE functional and the HSE06 functional, respectively. The band gaps are smaller than those of pristine monolayers, meaning that forming a heterostructure can evidently reduce the band gap and widen the range of absorption. Moreover, both the [Figures 2A,B](#) demonstrate that a type-II heterostructure is formed when ZnO comes into contact with C₂N.

[Figure 3](#) shows the electron transfer between two component layers. Work function (W_f) is a serious parameter defining the ability of a catalyst surface to attract electrons ([Vayenas et al., 1990](#)). The values of W_f for ZnO and C₂N are calculated as 4.82 eV and 5.78 eV, portending that electron flow from the ZnO layer to the C₂N layer at the interface. Electron migration from ZnO to C₂N is also observed from the planar-averaged charge density difference $\Delta\rho$ in [Figure 3B](#), which ceases until the Fermi level is aligned, producing the positively charged ZnO layer and the negatively charged C₂N layer. The visual charge density difference is also exhibited in [Figure 3B](#), in which the yellow and cyan marked areas represent electron accumulation and electron depletion, respectively. Therefore, a potential drop of 8.32 eV is formed in [Figure 3A](#). Finally, a built-in electric field, pointing from ZnO to C₂N, is generated at the interface. The Bader charge calculation ([Tang et al., 2009](#)) also demonstrates the

result of 0.203 electrons transferred from ZnO to C₂N. It is worth noting that the prominent potential drop in the ZnO/C₂N heterostructure can also offer a critical promotion for the separation of the photogenerated electron and hole, thereby reducing the recombination of carriers.

Suitable band edge positions (E_{VBM} and E_{CBM}) and decent band alignment are crucial for photocatalysis ([Zheng et al., 2018](#); [Tang et al., 2020](#)). The method proposed by [Toroker et al. \(2011\)](#) has been employed to evaluate the E_{VBM} and E_{CBM} of the ZnO/C₂N heterostructure so as to explore its potential as a photocatalyst. It is obvious from [Figure 3C](#) that both the E_{VBM} and E_{CBM} of the two monolayers ([Wang et al., 2018](#); [Zhang X. et al., 2019](#)) and the ZnO/C₂N heterostructure, meet the redox potential requirements for a photocatalyst in an acidic environment (pH = 0). The ZnO/C₂N heterostructure still has the talent of photocatalysis for water splitting in a neutral environment with pH = 7. Furthermore, a higher CBM and VBM of ZnO than those of C₂N can be observed. It is thus suggested that hydrogen evolution reaction (HER) occurs on the C₂N layer, while an oxygen evolution reaction (OER) happens on the ZnO layer. We then expand the type-II mechanism in the ZnO/C₂N heterostructure to boost HER and OER for water splitting. The conduction band offset (CBO) and valence band offset (VBO) are calculated as 0.98 eV and 0.69 eV, respectively. When the heterostructure is irradiated, the CBO promotes the transfer of photogenerated electrons in the CB of the ZnO layer to the CB of the C₂N layer. The photogenerated holes in the C₂N layer are driven by the VBO to the VB of the ZnO layer. Finally, the photogenerated electrons and holes remain in the C₂N and ZnO monolayers, respectively, bringing about carrier separation spatially. Naturally, the type-II band alignment of the ZnO/C₂N heterostructure is instrumental in overcoming the recombination of carriers to achieve better photocatalytic performance.

TABLE 1 Carrier mobilities of the ZnO/C₂N heterostructure and two monolayers.

Carrier	System	m_x^* (m_0)	m_y^* (m_0)	E_{1x} (eV)	E_{1y} (eV)	C_{2D_x} (N/m)	C_{2D_y} (N/m)	μ_x (cm ² /V/s)	μ_y (cm ² /V/s)
e	ZnO	0.21	0.25	5.91	5.38	51.76	51.65	477.8	406.1
	C ₂ N	0.46	0.42	1.59	2.58	160.45	160.57	4265.2	1944.5
	ZnO/ C ₂ N	0.14	0.14	7.36	5.85	205.78	205.66	2756.0	4359.9
h	ZnO	0.58	0.49	5.42	5.15	51.76	51.65	74.5	115.3
	C ₂ N	10.64	6.05	3.41	3.29	160.45	160.57	1.7	5.7
	ZnO/ C ₂ N	0.62	0.60	3.79	4.53	205.78	205.66	529.9	395.9

High carrier mobility μ is essential for superior photocatalysts (Guo et al., 2020; Ren et al., 2022b). The carrier mobility μ , defined as

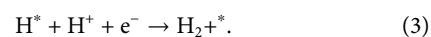
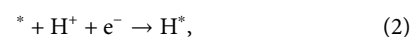
$$\mu = \frac{2e\hbar^3 C_{2D}}{3k_B T m^{*2} E_1^2} \quad (1)$$

has been evaluated based on the deformation potential theory (Bardeen and Shockley, 1950) for both the ZnO/C₂N heterostructure and the two monolayers. The methods and details are mentioned in Supplementary Section S1. As for the results of the ZnO monolayer listed in Table 1, the electron mobilities in the x - and y -directions are superior to those of the hole, conforming to previous theoretical (Ren et al., 2020) and experimental (Gonzalez-Valls and Lira-Cantu, 2009; Anta et al., 2012) results. It can be observed from Table 1 that the excellent electron mobilities of the C₂N monolayer are 4265 and 1944 cm²/V/s in the x - and y -directions, mainly due to the small carrier effective mass (m^*) and deformation potential constant (E_1). However, the hole m^* of the C₂N monolayer is several times that of the electron, resulting in low hole mobility (Kumar et al., 2018; Zhang X. et al., 2019).

The hole m^* s of the ZnO/C₂N heterostructure in the x - and y -directions are close to those of the ZnO monolayer, while the values of E_1 in the aforementioned directions are comparable to those of the C₂N monolayer. The in-plane stiffness (C_{2D}) of the ZnO/C₂N heterostructure increases and is about equal to the sum of two component layers. Consequently, the hole mobilities of the heterostructure in the x - and y -directions are 529.9 and 395.9 cm²/V/s, respectively, where pronounced improvements are due to the abovementioned changes of m^* , E_1 , and C_{2D} . It can be deduced that higher carrier mobility will induce enhanced carrier separation and migration in the ZnO/C₂N heterostructure, which should illuminate its photocatalytic prospects for application in water splitting.

In order to explore the kinetic behavior of water splitting, the Gibbs free energy difference ΔG of HER and OER on the ZnO/C₂N heterostructure is calculated using the method developed by Nørskov

et al. (2005). The calculation details and favor absorption sites are present in the Supplementary Material. The HER is divided into the following two reactions:



H^* is the only intermediate of HER, and it is obvious in Figure 4A that ΔG is a function of H coverage θ . When the θ equals 2/6, ΔG can be as low as 0.14 eV, which is comparable to the value of the C₂N/WS₂ heterostructure (Kumar et al., 2018). Therefore, the ZnO/C₂N heterostructure can be used as a potential photocatalyst for HER due to the small value of ΔG (Hinnemann et al., 2005).

The OER involves the following four steps:

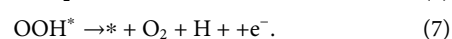
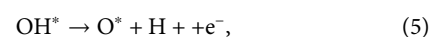
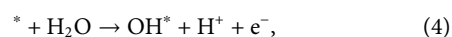


Figure 4B shows the first step, with an overpotential of 2.19 V, is the limiting step when no external potential is applied. Under the action of 1.23 V external potential, the overpotential reduces to 0.96 V. As the value of the extra potential increases to 2.19 V, all the OER steps are downhill, suggesting that these reaction steps are exothermic.

The performance of absorption is an important function of a photocatalyst, as it is the first step in water splitting to produce electron-hole pairs. Superior absorption with a wide range and a high coefficient is essential for a photocatalyst's effective solar energy utilization. The optical coefficients $\alpha(\omega)$ of the ZnO/C₂N heterostructure and two components are calculated with the following equation (Gajdoš et al., 2006):

$$\alpha(\omega) = \sqrt{2}\omega \left[\sqrt{\varepsilon_1(\omega)^2 + \varepsilon_2(\omega)^2} - \varepsilon_1(\omega) \right]^{1/2} \quad (8)$$

In this equation, ω_1 and ω_2 represent the real and imaginary parts of the dielectric function, respectively. The result, displayed in

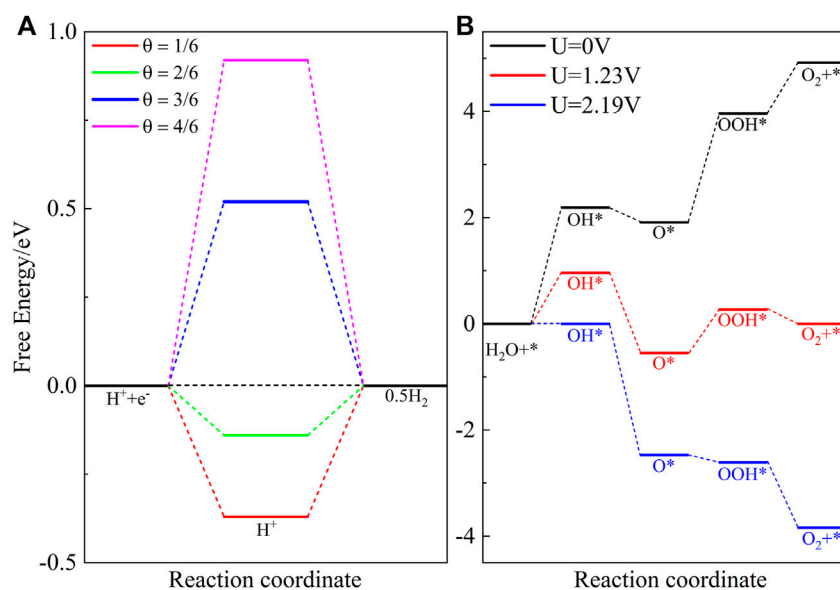


FIGURE 4
Free energy differences of (A) HER and (B) OER steps.

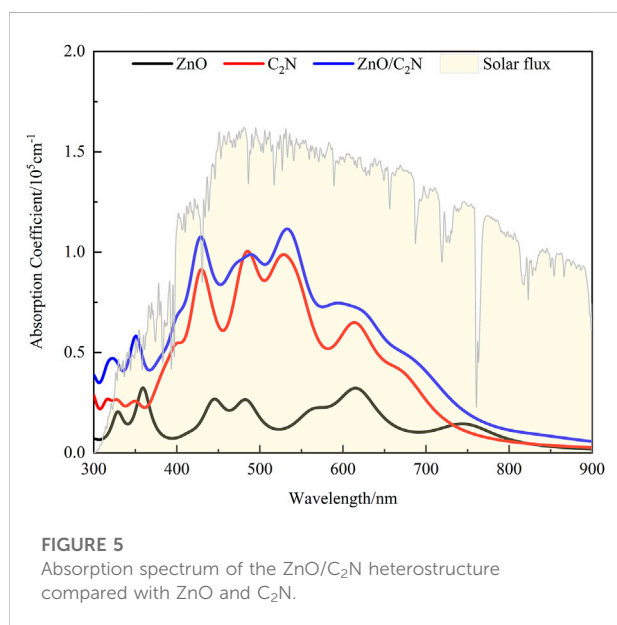


FIGURE 5
Absorption spectrum of the ZnO/C₂N heterostructure compared with ZnO and C₂N.

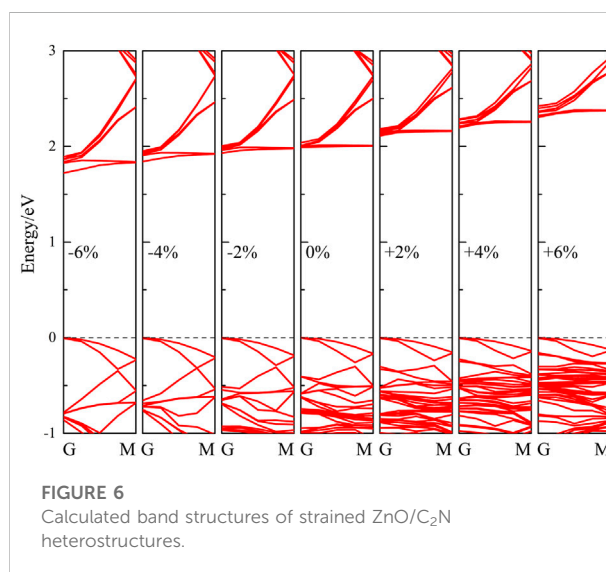


FIGURE 6
Calculated band structures of strained ZnO/C₂N heterostructures.

Figure 5, demonstrates the advantage of the heterostructure in absorption over ZnO and C₂N. The heterostructure not only possesses a higher absorption coefficient ($\sim 10^5 \text{cm}^{-1}$) than ZnO and C₂N but also has a wider absorption range from visible to ultraviolet light. The improvement in absorption performance can be attributed to its reduced band gap and significantly improved carrier mobility. The excellent absorption ability can generate more electron-hole pairs in the first step of water

splitting, which is beneficial for the ZnO/C₂N heterostructure in realizing its efficient photocatalytic performance.

The lateral strain is a common effect in heterostructures, as well as being a proven effective means of improving the photocatalytic performance of 2D material (Feng et al., 2012; Zhang J.-R. et al., 2019). We thus undertook a full investigation of the electronic and optical properties of the ZnO/C₂N heterostructure with biaxial lateral strain to explore the

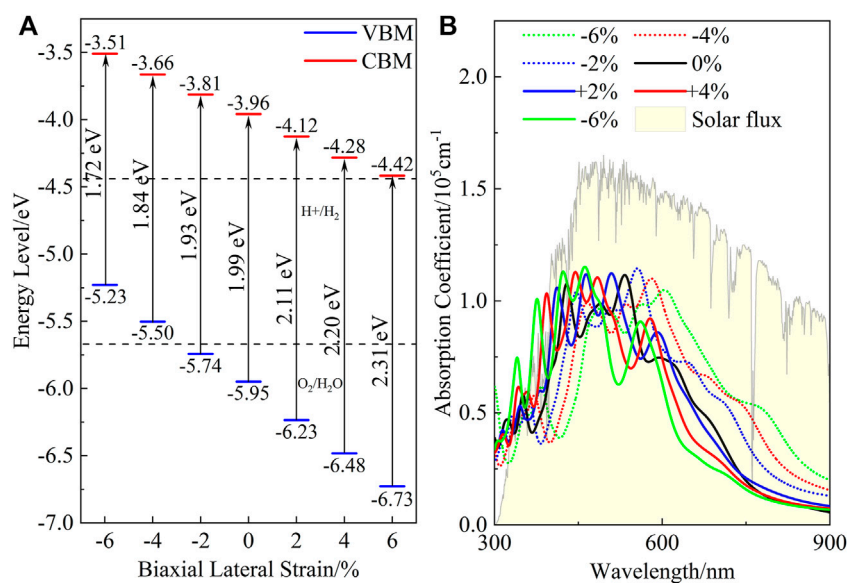


FIGURE 7

(A) Band alignment and (B) absorption spectrum of ZnO/C₂N heterostructure under different strain conditions.

regulatory effect of strain on photocatalytic performance. Strain ranging from -6% to $+6\%$ was applied to the ZnO/C₂N heterostructure, and the band structures calculated with the HSE06 functional in Figure 6 clearly announce the structure's identity as a direct band gap semiconductor.

Meanwhile, it can be seen from the PDOS exhibited in Supplementary Figure S13 that the strained heterostructures also belong to type-II heterostructures, as both the VBM and CBM of the ZnO are higher than those of C₂N. Moreover, it is clear in Figure 7A that compressive strain reduces the band gap, while tensile strain increases the gap. When the lattice is compressed by 6%, the band gap decreases to 1.72 eV, while the gap value increases to 2.31 eV when the heterostructure is expanded by 6%. Within the strain range of -2% to $+6\%$, we can also see that the band edge positions of the heterostructure still meet the requirements of photocatalysis for water splitting at the condition of pH = 0. It is very important for heterostructures to maintain their photocatalytic ability across a wide pH range (Ren et al., 2019). The band alignment shown in Supplementary Figure S15 indicates that the strained heterostructures still possess potential application for water splitting across a wide pH range. Figure 7B shows the effect of the strain on the absorption performance of the ZnO/C₂N heterostructure. Compared with the freestanding ZnO/C₂N heterostructure, the compressed heterostructures have higher absorption intensity and a wider absorption range, while the lattice expansion leads to improvement in the absorption performance of the heterostructures in the ultraviolet

range. The significant modification of absorption is mainly a benefit of the regulation of the band gap. All the results directly confirm that the ZnO/C₂N heterostructure is a promising candidate for use in the field of water splitting.

Conclusion

In this study, the electronic and absorption properties of the ZnO/C₂N heterostructure are explored to reveal its potential for water splitting. The stabilized heterostructure is given a reduced band gap of 1.99 eV, while its band edge positions also meet the water-splitting requirements. The band alignment of the heterostructure belongs to type-II, which leads to the generation of a built-in electrical field between the two layers that promote carrier separation and migration. The more significant change is that the carrier mobility of the ZnO/C₂N heterostructure is several times improved. The results of the Gibbs free energy calculation clearly indicate the promising catalytic ability of the ZnO/C₂N heterostructure. As for the optical absorption performance, the reduced band gap and excellent carrier mobility endow the ZnO/C₂N heterostructure with considerable absorption intensity and a wider absorption range. Moreover, the electronic and absorption properties of the ZnO/C₂N heterostructure can be substantially tuned with biaxial lateral strain. All the results confirm that the ZnO/C₂N heterostructure has potential use as a superior photocatalyst for water splitting.

Data availability statement

The original contributions presented in the study are included in the article/**Supplementary Material**, and further inquiries can be directed to the corresponding author.

Author contributions

All authors listed have made a substantial, direct, and intellectual contribution to the work and approved it for publication.

Funding

This work was financially supported by the National Natural Science Foundation of China (Grant No. 11875284), the Program for Science and Technology Innovation Talents in Universities of Henan Province (No. 21HASTIT020), and the Key Scientific Research Project of Colleges and Universities in Henan Province (No. 22A140023).

References

- Anta, J., Guillén, E., and Tena-Zaera, R. (2012). ZnO-based dye-sensitized solar cells. *J. Phys. Chem. C* 116 (21), 11413–11425. doi:10.1021/jp3010025
- Ashwin Kishore, M., and Ravindran, P. (2017). Tailoring the electronic band gap and band edge positions in the C₂N monolayer by P and as substitution for photocatalytic water splitting. *J. Phys. Chem. C* 121 (40), 22216–22224. doi:10.1021/acs.jpcc.7b07776
- Bafekry, A., Akgenc, B., Shayesteh, S., and Mortazavi, B. (2020). Tunable electronic and magnetic properties of graphene/carbon-nitride van der Waals heterostructures. *Appl. Surf. Sci.* 505, 144450. doi:10.1016/j.apsusc.2019.144450
- Bardeen, J., and Shockley, W. (1950). Deformation potentials and mobilities in non-polar crystals. *Phys. Rev.* 80 (1), 72. doi:10.1103/PhysRev.80.72
- Cheng, L., Li, X., Zhang, H., and Xiang, Q. (2019). Two-dimensional transition metal MXene-based photocatalysts for solar fuel generation. *J. Phys. Chem. Lett.* 10 (12), 3488–3494. doi:10.1021/acs.jpclett.9b00736
- Deng, D., Novoselov, K., Fu, Q., Zheng, N., Tian, Z., and Bao, X. (2016). Catalysis with two-dimensional materials and their heterostructures. *Nat. Nanotechnol.* 11 (3), 218–230. doi:10.1038/nnano.2015.340
- Du, J., Xia, C., Wang, T., Xiong, W., and Li, J. (2016). Modulation of the band structures and optical properties of holey C₂N nanosheets by alloying with group IV and V elements. *J. Mat. Chem. C* 4 (39), 9294–9302. doi:10.1039/C6TC02469F
- Fan, F., Wang, R., Zhang, H., and Wu, W. (2021). Emerging beyond-graphene elemental 2D materials for energy and catalysis applications. *Chem. Soc. Rev.* 50 (19), 10983–11031. doi:10.1039/C9CS00821G
- Fan, Y., Wang, J., and Zhao, M. (2019). Spontaneous full photocatalytic water splitting on 2D MoSe₂/SnSe₂ and WSe₂/SnSe₂ vdW heterostructures. *Nanoscale* 11 (31), 14836–14843. doi:10.1039/C9NR03469B
- Feng, J., Qian, X., Huang, C., and Li, J. (2012). Strain-engineered artificial atom as a broad-spectrum solar energy funnel. *Nat. Photonics* 6 (12), 866–872. doi:10.1038/nphoton.2012.285
- Fujishima, A., and Honda, K. (1972). Electrochemical photolysis of water at a semiconductor electrode. *Nature* 238 (5358), 37–38. doi:10.1038/238037a0
- Gajdoš, M., Hummer, K., Kresse, G., Furthmüller, J., and Bechstedt, F. (2006). Linear optical properties in the projector-augmented wave methodology. *Phys. Rev. B* 73 (4), 045112. doi:10.1103/PhysRevB.73.045112

Conflict of interest

The authors declare that the research was conducted in the absence of any commercial or financial relationships that could be construed as a potential conflict of interest.

Publisher's note

All claims expressed in this article are solely those of the authors and do not necessarily represent those of their affiliated organizations, or those of the publisher, the editors, and the reviewers. Any product that may be evaluated in this article, or claim that may be made by its manufacturer, is not guaranteed or endorsed by the publisher.

Supplementary material

The Supplementary Material for this article can be found online at: <https://www.frontiersin.org/articles/10.3389/fchem.2022.1048437/full#supplementary-material>

- Ganguly, P., Harb, M., Cao, Z., Cavallo, L., Breen, A., Dervin, S., et al. (2019). 2D nanomaterials for photocatalytic hydrogen production. *ACS Energy Lett.* 4 (7), 1687–1709. doi:10.1021/acscenergylett.9b00940
- Gonzalez-Valls, I., and Lira-Cantu, M. (2009). Vertically-aligned nanostructures of ZnO for excitonic solar cells: A review. *Energy Environ. Sci.* 2 (1), 19–34. doi:10.1039/B811536B
- Grimme, S., Antony, J., Ehrlich, S., and Krieg, H. (2010). A consistent and accurate *ab initio* parametrization of density functional dispersion correction (DFT-D) for the 94 elements H-Pu. *J. Chem. Phys.* 132 (15), 154104. doi:10.1063/1.3382344
- Guan, S., Cheng, Y., Liu, C., Han, J., Lu, Y., Yang, S., et al. (2015). Effects of strain on electronic and optic properties of holey two-dimensional C₂N crystals. *Appl. Phys. Lett.* 107 (23), 231904. doi:10.1063/1.4937269
- Guo, H., Zhang, Z., Huang, B., Wang, X., Niu, H., Guo, Y., et al. (2020). Theoretical study on the photocatalytic properties of 2D InX (X= S, Se)/transition metal disulfide (MoS₂ and WS₂) van der Waals heterostructures. *Nanoscale* 12 (38), 20025–20032. doi:10.1039/D0NR04725B
- Guo, Z., Miao, N., Zhou, J., Sa, B., and Sun, Z. (2017). Strain-mediated type-I/type-II transition in MXene/Blue phosphorene van der Waals heterostructures for flexible optical/electronic devices. *J. Mat. Chem. C* 5 (4), 978–984. doi:10.1039/C6TC04349F
- Heyd, J., Scuseria, G., and Ernzerhof, M. (2003). Hybrid functionals based on a screened Coulomb potential. *J. Chem. Phys.* 118 (18), 8207–8215. doi:10.1063/1.1564060
- Hinnemann, B., Moses, P., Bonde, J., Jørgensen, K., Nielsen, J., Horch, S., et al. (2005). Biomimetic hydrogen evolution: MoS₂ nanoparticles as catalyst for hydrogen evolution. *J. Am. Chem. Soc.* 127 (15), 5308–5309. doi:10.1021/ja0504690
- Kishore, M., Sjastad, A., and Ravindran, P. (2019). Influence of hydrogen and halogen adsorption on the photocatalytic water splitting activity of C₂N monolayer: A first-principles study. *Carbon* 141, 50–58. doi:10.1016/j.carbon.2018.08.072
- Kresse, G., and Furthmüller, J. (1996a). Efficiency of *ab-initio* total energy calculations for metals and semiconductors using a plane-wave basis set. *Comput. Mat. Sci.* 6 (1), 15–50. doi:10.1016/0927-0256(96)00008-0
- Kresse, G., and Furthmüller, J. (1996b). Efficient iterative schemes for *ab initio* total-energy calculations using a plane-wave basis set. *Phys. Rev. B* 54 (16), 11169–11186. doi:10.1103/PhysRevB.54.11169

- Kumar, R., Das, D., and Singh, A. (2018). C₂N/WS₂ van der Waals type-II heterostructure as a promising water splitting photocatalyst. *J. Catal.* 359, 143–150. doi:10.1016/j.jcat.2018.01.005
- Lee, J., Sorescu, D., and Deng, X. (2016). Tunable lattice constant and band gap of single- and few-layer ZnO. *J. Phys. Chem. Lett.* 7 (7), 1335–1340. doi:10.1021/acs.jpclett.6b00432
- Li, X., Yu, J., and Jaroniec, M. (2016). Hierarchical photocatalysts. *Chem. Soc. Rev.* 45 (9), 2603–2636. doi:10.1039/C5CS00838G
- Luo, X., Wang, G., Huang, Y., Wang, B., Yuan, H., and Chen, H. (2017). A two-dimensional layered CdS/C₂N heterostructure for visible-light-driven photocatalysis. *Phys. Chem. Chem. Phys.* 19 (41), 28216–28224. doi:10.1039/C7CP04108J
- Ma, Z., Wang, S., Li, C., and Wang, F. (2021). Strain engineering for C₂N/Janus monochalcogenides van der Waals heterostructures: Potential applications for photocatalytic water splitting. *Appl. Surf. Sci.* 536, 147845. doi:10.1016/j.apsusc.2020.147845
- Mahmood, J., Lee, E., Jung, M., Shin, D., Jeon, I., Jung, S., et al. (2015). Nitrogenated holey two-dimensional structures. *Nat. Commun.* 6 (1), 6486–6487. doi:10.1038/ncomms7486
- Momma, K., and Izumi, F. (2011). VESTA3 for three-dimensional visualization of crystal, volumetric and morphology data. *J. Appl. Crystallogr.* 44 (6), 1272–1276. doi:10.1107/S0021889811038970
- Monkhorst, H., and Pack, J. (1976). Special points for Brillouin-zone integrations. *Phys. Rev. B* 13 (12), 5188–5192. doi:10.1103/PhysRevB.13.5188
- Nørskov, J., Bligaard, T., Logadottir, A., Kitchin, J., Chen, J., Pandelov, S., et al. (2005). Trends in the exchange current for hydrogen evolution. *J. Electrochem. Soc.* 152 (3), J23. doi:10.1149/1.1856988
- Novoselov, K., Mishchenko, A., Carvalho, A., and Castro Neto, A. (2016). 2D materials and van der Waals heterostructures. *Science* 353 (6298), aac9439. doi:10.1126/science.aac9439
- Perdew, J., Burke, K., and Ernzerhof, M. (1996). Generalized gradient approximation made simple. *Phys. Rev. Lett.* 77 (18), 3865–3868. doi:10.1103/PhysRevLett.77.3865
- Qin, H., Ren, K., Zhang, G., Dai, Y., and Zhang, G. (2022). Lattice thermal conductivity of Janus MoSSe and WSSe monolayers. *Phys. Chem. Chem. Phys.* 24 (34), 20437–20444. doi:10.1039/D2CP01692C
- Ren, K., Chen, Y., Qin, H., Feng, W., and Zhang, G. (2022a). Graphene/biphenylene heterostructure: Interfacial thermal conduction and thermal rectification. *Appl. Phys. Lett.* 121 (8), 082203. doi:10.1063/5.0100391
- Ren, K., Ren, C., Luo, Y., Xu, Y., Yu, J., Tang, W., et al. (2019). Using van der Waals heterostructures based on two-dimensional blue phosphorus and XC (X = Ge, Si) for water-splitting photocatalysis: A first-principles study. *Phys. Chem. Chem. Phys.* 21 (19), 9949–9956. doi:10.1039/C8CP07680D
- Ren, K., Yan, Y., Zhang, Z., Sun, M., and Schwingschögl, U. (2022b). A family of Li_xB₂ monolayers with a wide spectrum of potential applications. *Appl. Surf. Sci.* 604, 154317. doi:10.1016/j.apsusc.2022.154317
- Ren, K., Yu, J., and Tang, W. (2020). Two-dimensional ZnO/BSe van der Waals heterostructure used as a promising photocatalyst for water splitting: A dft study. *J. Alloys Compd.* 812, 152049. doi:10.1016/j.jallcom.2019.152049
- Roger, I., Shipman, M., and Symes, M. (2017). Earth-abundant catalysts for electrochemical and photoelectrochemical water splitting. *Nat. Rev. Chem.* 1 (1), 0003–0013. doi:10.1038/s41570-016-0003
- Sahin, H. (2015). Structural and phononic characteristics of nitrogenated holey graphene. *Phys. Rev. B* 92 (8), 085421. doi:10.1103/PhysRevB.92.085421
- Song, J., Zheng, H., Liu, M., Zhang, G., Ling, D., and Wei, D. (2021). A first-principles study on the electronic and optical properties of a type-II C₂N/g-ZnO van der Waals heterostructure. *Phys. Chem. Chem. Phys.* 23 (6), 3963–3973. doi:10.1039/D1CP00122A
- Tang, W., Sanville, E., and Henkelman, G. (2009). A grid-based Bader analysis algorithm without lattice bias. *J. Phys. Condens. Matter* 21 (8), 084204. doi:10.1088/0953-8984/21/8/084204
- Tang, Y., Liu, M., Zhou, Y., Ren, C., Zhong, X., and Wang, J. (2020). First-principles prediction of facet-dependent electronic and optical properties in InSe/GaAs heterostructure with potential in solar energy utilization. *J. Alloys Compd.* 842, 155901. doi:10.1016/j.jallcom.2020.155901
- Toroker, M., Kanan, D., Alidoust, N., Isseroff, L., Liao, P., and Carter, E. (2011). First principles scheme to evaluate band edge positions in potential transition metal oxide photocatalysts and photoelectrodes. *Phys. Chem. Chem. Phys.* 13 (37), 16644–16654. doi:10.1039/C1CP22128K
- Vayenas, C., Bebelis, S., and Ladas, S. (1990). Dependence of catalytic rates on catalyst work function. *Nature* 343 (6259), 625–627. doi:10.1038/343625a0
- Voiry, D., Yang, J., and Chhowalla, M. (2016). Recent strategies for improving the catalytic activity of 2D TMD nanosheets toward the hydrogen evolution reaction. *Adv. Mat.* 28 (29), 6197–6206. doi:10.1002/adma.201505597
- Wang, B., Yuan, H., Chang, J., Chen, X., and Chen, H. (2019). Two dimensional InSe/C₂N van der Waals heterojunction as enhanced visible-light-responsive photocatalyst for water splitting. *Appl. Surf. Sci.* 485, 375–380. doi:10.1016/j.apsusc.2019.03.344
- Wang, G., Chang, J., Tang, W., Xie, W., and Ang, Y. S. (2022). 2D materials and heterostructures for photocatalytic water-splitting: A theoretical perspective. *J. Phys. D: Appl. Phys.* 55 (29), 293002. doi:10.1088/1361-6463/ac5771
- Wang, G., Li, Z., Wu, W., Guo, H., Chen, C., Yuan, H., et al. (2020a). A two-dimensional h-BN/C₂N heterostructure as a promising metal-free photocatalyst for overall water-splitting. *Phys. Chem. Chem. Phys.* 22 (42), 24446–24454. doi:10.1039/D0CP03925J
- Wang, S., Ren, C., Tian, H., Yu, J., and Sun, M. (2018). MoS₂/ZnO van der Waals heterostructure as a high-efficiency water splitting photocatalyst: A first-principles study. *Phys. Chem. Chem. Phys.* 20 (19), 13394–13399. doi:10.1039/C8CP00808F
- Wang, V., Xu, N., Liu, J., Tang, G., and Geng, W. (2021). Vaspkit: A user-friendly interface facilitating high-throughput computing and analysis using VASP code. *Comput. Phys. Commun.* 267, 108033. doi:10.1016/j.cpc.2021.108033
- Wang, X., Maeda, K., Thomas, A., Takanabe, K., Xin, G., Carlsson, J., et al. (2009). A metal-free polymeric photocatalyst for hydrogen production from water under visible light. *Nat. Mat.* 8 (1), 76–80. doi:10.1038/nmat2317
- Wang, X., Wang, Y., Quhe, R., Tang, Y., Dai, X., and Tang, W. (2020b). Designing strained C₂N/GaTe (InTe) heterostructures for photovoltaic and photocatalytic application. *J. Alloys Compd.* 816, 152559. doi:10.1016/j.jallcom.2019.152559
- Xu, B., Xiang, H., Wei, Q., Liu, J., Xia, Y., Yin, J., et al. (2015). Two-dimensional graphene-like C₂N: An experimentally available porous membrane for hydrogen purification. *Phys. Chem. Chem. Phys.* 17 (23), 15115–15118. doi:10.1039/C5CP01789K
- Ye, K., Li, H., Huang, D., Xiao, S., Qiu, W., Li, M., et al. (2019). Enhancing photoelectrochemical water splitting by combining work function tuning and heterojunction engineering. *Nat. Commun.* 10 (1), 3687–3689. doi:10.1038/s41467-019-11586-y
- Zhang, H., Zhang, X., Yang, G., and Zhou, X. (2018). Point defect effects on photoelectronic properties of the potential metal-free C₂N photocatalysts: Insight from first-principles computations. *J. Phys. Chem. C* 122 (10), 5291–5302. doi:10.1021/acs.jpcc.7b12428
- Zhang, J.-R., Deng, X., Gao, B., Chen, L., Au, C., Li, K., et al. (2019a). Theoretical study on the intrinsic properties of In₂Se₃/MoS₂ as a photocatalyst driven by near-infrared, visible and ultraviolet light. *Catal. Sci. Technol.* 9 (17), 4659–4667. doi:10.1039/C9CY00997C
- Zhang, J., Zhang, C., Ren, K., Lin, X., and Cui, Z. (2022). Tunable electronic and magnetic properties of Cr₂Ge₂Te₆ monolayer by organic molecular adsorption. *Nanotechnology* 33 (34), 345705. doi:10.1088/1361-6528/ac715d
- Zhang, X., Chen, A., Zhang, Z., Jiao, M., and Zhou, Z. (2019b). Rational design of C₂N-based type-II heterojunctions for overall photocatalytic water splitting. *Nanoscale Adv.* 1 (1), 154–161. doi:10.1039/C8NA00084K
- Zhao, D., Wang, Y., Dong, C., Huang, Y., Chen, J., Xue, F., et al. (2021). Boron-doped nitrogen-deficient carbon nitride-based Z-scheme heterostructures for photocatalytic overall water splitting. *Nat. Energy* 6 (4), 388–397. doi:10.1038/s41560-021-00795-9
- Zheng, B., Ma, C., Li, D., Lan, J., Zhang, Z., Sun, X., et al. (2018). Band alignment engineering in two-dimensional lateral heterostructures. *J. Am. Chem. Soc.* 140 (36), 11193–11197. doi:10.1021/jacs.8b07401